

Reinforcement Learning with Verifiable yet Noisy Rewards under Imperfect Verifiers

Xin-Qiang Cai¹ Wei Wang^{2,1} Feng Liu² Tongliang liu³

Gang Niu¹ Masashi Sugiyama^{1,2}

¹RIKEN AIP, Tokyo, Japan ²The University of Tokyo, Tokyo, Japan

³The University of Melbourne, Melbourne, Australia

⁴The University of Sydney, Sydney, Australia

Abstract

Reinforcement Learning with Verifiable Rewards (RLVR) replaces costly human labeling with automated verifiers. To reduce verifier hacking, many RLVR systems binarize rewards to $\{0, 1\}$, but imperfect verifiers inevitably introduce *false negatives* (rejecting correct answers) and *false positives* (accepting incorrect ones). We formalize verifier unreliability as a stochastic reward channel with asymmetric noise rates ρ_0 and ρ_1 —the FP rate and the FN rate, respectively. From this abstraction we derive two lightweight corrections: (i) a *backward* correction that yields an unbiased surrogate reward and thus an unbiased policy-gradient estimator in expectation, and (ii) a *forward* correction that reweights score-function terms so the expected update aligns with the clean gradient direction and requires only the FN rate. We implement both as lightweight hooks in a group relative policy optimization pipeline, both corrections improve RLVR for math reasoning under synthetic and real verifier noise, with the forward variant being more stable under heavier noise. Finally, an appeals mechanism with a lightweight LLM verifier estimates the FN rate online and further improves performance.

1. Introduction

Reinforcement Learning with Verifiable Rewards (RLVR) offers a scalable paradigm for improving the reasoning abilities of Large Language Models (LLMs) by replacing expensive human annotation with automated feedback [31]. In this problem, a policy is trained using rewards from a verifier that automatically checks the correctness of a model’s output [22]. The efficacy of this

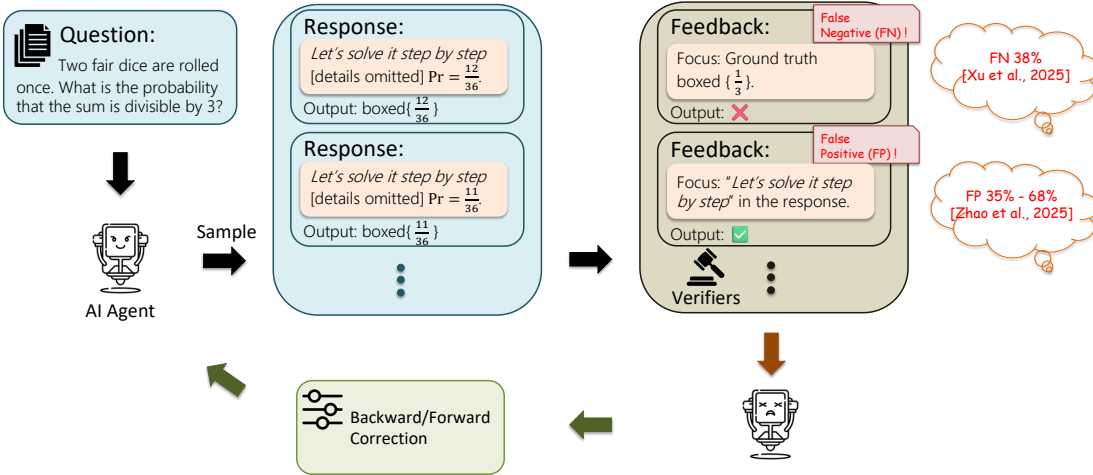


Figure 1: Verifier-noise flow in RLVR. An AI agent produces candidate solutions that are scored by automated verifiers. While verifiers would yield *false negatives* ($\frac{12}{36}$ vs. $\frac{1}{3}$, reaching 38% rates [33]) and *false positives* (mislead by “Let’s solve it step by step...”, reaching 35% – 68% rates [35]), confusing the agent; applying our backward/forward corrections restores correct signals.

approach, however, heavily depends on the verifier’s reliability. Emerging evidence reveals that verifiers are systematically fallible in two critical ways: they can accept incorrect solutions (*false positives*; *FPs*) or reject correct ones (*false negatives*; *FNs*) [33, 35].

FPs have been widely documented as a vulnerability of LLM-based verifiers. Recent studies showed that LLM judges can be swayed by superficial cues—e.g., popular specialized verifiers, such as GPT-4o, give 35 % – 66.8% FP rate when the answer starts with *Let’s solve this problem step by step* [35, 24, 23, 1]. Conversely, *FNs* are common with rule-based verifiers. These checkers, while highly precise, are often brittle; they may reject valid solutions that are formatted differently, expressed in an algebraically equivalent form, or embedded in explanatory text [7]. A recent analysis of a math-RL dataset found that over 38% of responses flagged as incorrect by a rule-based system were in fact correct, a gap that a lightweight LLM verifier could partially close [33]. Both FPs and FNs materially degrade RLVR training: FNs deprive the agent of informative gradients and slow convergence, while FPs reward hackable patterns and inflate returns during policy optimization [33, 6].

Motivated by this asymmetry, we address these challenges by explicitly *treating verifier errors as noise* in the reward signal. We model the verifier as a stochastic reward channel that corrupts

the true, latent reward with verifier-conditional probabilities—the FP rate and the FN rate. Building on this formulation, we derive two estimators to counteract this noise. Our first method, *noisy Policy Gradient with Backward Correction (PGBC)*, inverts the noise process to compute an unbiased estimator of the true reward, which can be used as a drop-in replacement in any advantage-estimation in RL. Our second method, *noisy Policy Gradient with Forward Correction (PGFC)*, directly reweights the terms of the policy gradient to ensure its expected direction aligns with the clean gradient. This approach requires only an estimate of the FN rate to achieve directional correctness, making it suitable for the often harder-to-estimate FP rate [33]. The pipeline is illustrated in Figure 1.

We integrate these corrections into a group relative policy optimization (GRPO) [22]-based RLVR pipeline and demonstrate their effectiveness on competitive math reasoning benchmarks [22]. Both methods consistently outperform uncorrected training and achieve performance nearly equivalent to that of noise-free scenarios, with the forward correction offering the fastest and most stable convergence. We also propose a practical online estimation scheme for the FN rate: a querying mechanism where a low-cost LLM verifier like TinyV [33] re-evaluates outputs rejected by a primary rule-based checker. This hybrid approach provides a reliable estimate of the FN rate with minimal computational overhead, recovering near-oracle performance. Our contributions are: (i) a formal verifier-channel model for RLVR that captures the prevalent FP and FN errors; (ii) backward and forward corrections derived from RL principles to calibrate policy learning; and (iii) a practical implementation for online noise estimation that makes these corrections viable in real-world systems.

2. Related Works

Reasoning with LLMs. A large body of work improves LLM reasoning through prompting and search at inference time. Chain-of-Thought (CoT) prompting elicits step-by-step rationales and boosts arithmetic and commonsense reasoning [30], while self-consistency aggregates diverse reasoning paths to further improve robustness [29]. Decomposition-based prompting, such as Least-to-Most, solves complex problems via ordered sub-problems [36]; search-based schemes like Tree-of-Thoughts explicitly explore and evaluate alternative reasoning branches [34]. Orthogonally, training-time verifier signals can be used to re-rank candidate solutions, as in Cobbe et al. [2].

Our work is complementary: rather than proposing a new inference-time strategy or re-ranking scheme, we address *how* to perform *policy optimization* when the reward itself—supplied by a verifier—is noisy.

RLVR and verifier reliability. Recent math-RL pipelines combine on-policy RL (e.g., GRPO) with programmatic or LLM-based verifiers to yield verifiable rewards [18]. However, LLM-as-a-judge is prone to systematic biases, including position bias and prompt-based attacks, producing *FPs* (accepting incorrect solutions) [3, 27, 24, 35, 23]. Conversely, exact-match or brittle parsers in rule-based checkers can miss algebraic equivalences and text-formatted answers, leading to widespread *FNs* [14, 6]. A recent study showed that over 38% of model responses labeled incorrect by a rule-based pipeline were in fact correct, and introduced a lightweight verifier (TinyV) that recovers many such cases with minimal overhead [33]. Prior efforts therefore improved the *verifier* (e.g., better judges or appeals) or evaluation suites; in contrast, we treat verifier errors as verifier-conditional noise and directly *correct the policy gradient* so that learning remains aligned with the clean objective even when the verifier is imperfect.

Learning with noisy labels. While our method is derived from RL, it shares intuition with the literature on learning with label noise. Wang et al. [28] modeled reward corruption via a class-conditional confusion matrix and derived an unbiased surrogate reward for Q-learning algorithms to solve control tasks. In supervised learning, a central thread is to make empirical-risk minimization robust either by *correcting the loss* given a noise-transition model or by *avoiding* or *down-weighting* suspected noisy examples [25, 13]. The former includes the unbiased-risk estimators of Natarajan et al. [19] and the now-standard loss corrections of Patrini et al. [21]. A second family avoids the noise explicitly by relying on the “small-loss first” memorization dynamics of deep nets: mentor methods (MentorNet) learn a weighting network that feeds cleaner samples to the student, and *Co-teaching* [4] trains two peers that exchange their selected small-loss examples; semi-supervised hybrids such as *DivideMix* [12] split data into clean/noisy partitions via mixture modeling and co-train with consistency regularization [9]. Unlike them, we target the *policy gradient estimator* in RLVR: we instantiate both backward and forward corrections inside the policy gradient estimator to stabilize and align RL under verifier noise.

3. Problem Setup and Algorithms

In this section, we introduce the problem formulations and our proposed algorithms.

3.1. Problem Setup

We consider the standard RLVR setting where a stochastic policy $\pi_\theta(y|x)$ generates a response y for a given prompt x , where θ denotes learnable parameters. The goal is to maximize an objective based on the true, or *clean*, reward $R^*(x, y) \in \{0, 1\}$, which indicates whether the response y is genuinely correct. This objective is typically regularized by a KL-divergence term to a reference policy π_{ref} to maintain stability:

$$\begin{aligned} \max_{\theta} J_\beta(\theta) = \\ \mathbb{E}_x \mathbb{E}_{y \sim \pi_\theta(\cdot|x)} \left[R^*(x, y) - \beta \text{KL}(\pi_\theta(\cdot|x) \parallel \pi_{\text{ref}}(\cdot|x)) \right], \end{aligned} \quad (1)$$

in which KL denotes the Kullback-Leibler (KL)-divergence. The policy gradient with respect to the unregularized reward is given by the REINFORCE estimator [26], $\nabla_\theta J(\theta) = \mathbb{E}[R^*(x, y) \sum_t G_t]$, where $G_t = \nabla_\theta \log \pi_\theta(y_t | x, y_{<t})$ is the score function for the token at step t , and $y_{<t}$ denotes the sequence of tokens generated prior to step t . In the following, we will denote $R(x, y)$ with R for brevity.

In practice, the clean reward R^* is unavailable. Instead, the agent receives a noisy reward $\tilde{R}(x, y) \in \{0, 1\}$ from an automated verifier. We model this verifier as a stochastic *reward channel* that flips the latent clean reward to an observed noisy one. This channel is characterized by asymmetric, verifier-conditional noise rates.

Definition 1 (Verifier Reward Channel). The observed verifier reward \tilde{R} is generated from the latent clean reward R^* according to the following conditional probabilities:

$$\mathbb{P}(\tilde{R} = 1 | R^* = 0) = \rho_0,$$

$$\mathbb{P}(\tilde{R} = 0 | R^* = 1) = \rho_1,$$

where $\rho_0 + \rho_1 < 1$.

Assumptions and scope of the verifier channel. Definition 1 is a deliberately lightweight abstraction of verifier unreliability. It assumes (i) *instance-independent* class-conditional noise rates (ρ_0, ρ_1) that do not vary with (x, y) , and (ii) *conditional independence*: given the latent correctness $R^*(x, y)$, the verifier’s stochastic flip \tilde{R} is independent of the policy’s sampling randomness (hence independent of the score-function terms used by policy gradients). These assumptions are standard in class-conditional noise models and allow closed-form reward/gradient corrections. In real RLVR deployments, verifier errors can be content-dependent (e.g., spurious phrases can increase FPs), which violates (i) and can partially violate (ii). We therefore view (ρ_0, ρ_1) as *effective* noise rates, and empirically test robustness to mis-specification in Section 4.4; we further estimate ρ_1 online via a low-cost appeals mechanism in Section 4.3.

Based on this noise model, we establish a linear relationship between the expected noisy reward and the clean reward, which is presented in Proposition 1.

Proposition 1 (Connection between Corrupted Rewards and True Rewards). *Under the Verifier Reward Channel model, the expectation of the noisy reward \tilde{R} conditioned on the clean reward R^* is an affine transformation of R^* :*

$$\mathbb{E}[\tilde{R} | R^*] = (1 - \rho_0 - \rho_1) R^* + \rho_0.$$

The proof is provided in Appendix C.1. The central challenge of RLVR is that naively optimizing with the noisy reward \tilde{R} leads to a biased policy gradient, causing the policy to learn from mistakes of the verifier. Our goal is to develop policy gradient estimators that use only the observable noisy reward \tilde{R} but the expectation is either identical or parallel to the true policy gradient $\nabla_\theta J(\theta)$. We integrate these estimators within REINFORCE-style policy gradient algorithms widely used for reasoning tasks that compute normalized advantages over a group of sampled trajectories [22].

3.2. Noisy Policy Gradient with Backward Correction (PGBC)

Our first proposed approach aims to construct an unbiased estimator of the true reward R^* by “inverting” the noise process. Since the expected noisy reward $\mathbb{E}[\tilde{R} | R^*]$ is an affine transformation of the clean reward R^* in Proposition 1, we can solve for R^* to derive a corrected reward estimator, \hat{R} , that is unbiased in expectation.

Algorithm 1 Noisy Policy Gradient with Backward Correction (PGBC)

- 1: **Input:** Initial policy θ_0 ; learning rate η ; batch size M ; estimates of noise rates, $(\hat{\rho}_0, \hat{\rho}_1)$.
- 2: **loop**
- 3: Roll out M trajectories $\{(x_i, y_i)\}_{i=1}^M$, obtaining observed rewards $\{\tilde{R}_i\}_{i=1}^M$.
- 4: For each trajectory i , compute the unbiased reward estimate:
$$\hat{R}_i \leftarrow \frac{\tilde{R}_i - \hat{\rho}_0}{1 - \hat{\rho}_0 - \hat{\rho}_1}.$$
- 5: Compute the policy gradient using the corrected rewards $\{\hat{R}_i\}_{i=1}^M$.
- 6: Update parameters: $\theta \leftarrow \theta + \eta \Delta\theta$.
- 7: **end loop**

Theorem 1 (Unbiased Reward Estimator). *Given the verifier channel with known noise rates ρ_0 and ρ_1 with $\rho_0 + \rho_1 < 1$, the estimator*

$$\hat{R} = \frac{\tilde{R} - \rho_0}{1 - \rho_0 - \rho_1} \quad (2)$$

is an unbiased estimator of the true reward $R^(x, y)$, i.e., $\mathbb{E}[\hat{R}] = R^*$.*

The proof is provided in Appendix C.2. Theorem 1 shows that, by replacing the noisy reward \tilde{R} with \hat{R} in any standard policy gradient formulation, we obtain an unbiased estimate of the true policy gradient. This allows \hat{R} to serve as a drop-in replacement for the reward signal in complex RL algorithms, seamlessly integrating with advantage estimation and other machinery. The details of the algorithm are summarized in Algorithm 1. After rolling out a set of trajectories and obtaining their rewards, we use the corrected rewards to compute the policy gradients for model update.

3.3. Noisy Policy Gradient with Forward Correction (PGFC)

While PGBC provides an elegant unbiased estimator, it faces two practical challenges. First, the denominator $(1 - \rho_0 - \rho_1)$ can be small if the total noise rate is high, leading to high variance in the reward estimate \hat{R} and potentially unstable training. Second, it requires accurate estimation of both the false positive rate ρ_0 and the false negative rate ρ_1 , which are usually difficult to obtain in practice. The PGFC approach is introduced to mitigate these issues.

Instead of correcting the reward itself, this method directly modifies the policy gradient estimator to ensure its expectation is correctly aligned. The core idea is to reweight the score function G_t under the t -th token based on the observed noisy reward \tilde{R} . We define an update term $h_t = w_{\tilde{R}} G_t$ and choose the *forward weights* w_0 (for $\tilde{R} = 0$) and w_1 (for $\tilde{R} = 1$) such that the expected update $\mathbb{E}[h_t]$ is parallel to the clean gradient $\nabla_{\theta} J(\theta)$. The key insight is to choose the forward weights so that the conditional expectations given the true reward R^* have a specific structure.

Proposition 2 (Conditional Expectation of Forward Weights). *Let the forward weights be defined as $w_0 = \rho_1 - 1$ and $w_1 = \rho_1$. Under the Verifier Reward Channel model, the conditional expectations of the corresponding weight $w_{\tilde{R}}$ given the true reward R^* are:*

1. $\mathbb{E}[w_{\tilde{R}} | R^* = 1] = 0$.
2. $\mathbb{E}[w_{\tilde{R}} | R^* = 0] = -(1 - \rho_0 - \rho_1)$.

The proof can be found in Appendix C.3. Proposition 2 reveals that, in expectation, the forward weights are chosen so that their conditional expectation vanishes when $R^* = 1$, i.e., truly positive cases do not require correction. Consequently, the explicit contribution to the correction term arises from samples with $R^* = 0$. This structure allows us to recover the correct gradient direction, as shown in the following theorem.

Theorem 2 (Policy Gradient Correction with Only ρ_1). *Let the gradient-update term be $\Delta\theta = \frac{1}{M} \sum w_{\tilde{R}} G_t$, where $w_0 = \rho_1 - 1$ and $w_1 = \rho_1$ with M trajectories. Under the Verifier Reward Channel model, the expected update is parallel to the clean policy gradient:*

$$\mathbb{E}[\Delta\theta] = c \nabla_{\theta} J(\theta), \quad (3)$$

in which $c = (1 - \rho_0 - \rho_1)$.

The proof is given in Appendix C.4. Since $1 - \rho_0 - \rho_1 > 0$, Theorem 2 guarantees that the expected update of the policy is in the same direction as the true gradient; meanwhile, the positive scaling factor $(1 - \rho_0 - \rho_1)$ can be absorbed into the learning rate. By avoiding the inverse operation of PGBC, PGFC circumvents the variance-inflation problem. Furthermore, its reliance solely on the FN rate makes it more practical, as the FN rate is often the more dominant and easily estimable error source in RLVR with rule-based verifiers [33].

In practice, we estimate $\hat{\rho}_1$ during training by *appealing* a small, uniformly random subset of rule-based negatives to a lightweight LLM verifier (e.g., TinyV [33]) and then smoothing the empirical

Algorithm 2 Noisy Policy Gradient with Forward Correction (PGFC)

- 1: **Input:** Initial policy θ_0 ; learning rate η ; batch size M ; an estimate of the false negative rate, $\hat{\rho}_1$.
- 2: **loop**
- 3: Roll out M trajectories and observe rewards $\{\tilde{R}_i\}_{i=1}^M$.
- 4: For each trajectory i , define the weight based on the observed reward \tilde{R}_i :
$$w_{\tilde{R}_i} \leftarrow \begin{cases} \hat{\rho}_1 - 1, & \text{if } \tilde{R}_i = 0, \\ \hat{\rho}_1, & \text{if } \tilde{R}_i = 1. \end{cases}$$
- 5: For each trajectory i , compute the score-function term G_i and the weighted term $h_i \leftarrow w_{\tilde{R}_i} G_i$.
- 6: Form the policy gradient estimate: $\hat{g} \leftarrow \frac{1}{M} \sum_{i=1}^M h_i$.
- 7: Update parameters: $\theta \leftarrow \theta + \eta \hat{g}$.
- 8: **end loop**

flip rate. Concretely, at step t , let $\mathcal{N}_R^{(t)}$ be items labeled negative by the rule-based verifier, $\mathcal{P}_R^{(t)}$ the rule-based positives, and sample a fraction $q \in (0, 1]$ of $\mathcal{N}_R^{(t)}$ for appeal; denote by $\mathcal{P}_L^{(t)}$ those appealed items that the LLM flips to positive (i.e., rule-negative & LLM-positive). Using a Horvitz–Thompson correction [10], we estimate the FN rate as $|\mathcal{P}_L^{(t)}|/q$ and the true positive (TP) rate as $|\mathcal{P}_R^{(t)}|$ (since the rule-based FP rate should be 0). We then set $\hat{\rho}_1^{(t)} = \frac{|\mathcal{P}_L^{(t)}|/q + \alpha}{|\mathcal{P}_L^{(t)}|/q + |\mathcal{P}_R^{(t)}| + \alpha + \beta}$ with small Beta-prior pseudocounts α, β (we use 10^{-5}), and apply exponential moving average (EMA) smoothing over a sliding window. If both $\hat{\rho}_0$ and $\hat{\rho}_1$ are available, one can use PGBC; if only $\hat{\rho}_1$ is available, use PGFC. The code can be found in <https://github.com/caixq1996/noisy-RLVR>. More details of appealing mechanism can be found in Appendix D.4.

Bridging REINFORCE-Style Corrections to GRPO Updates. Our core analysis (Theorems 1 and 2) is stated for REINFORCE-style policy gradients. In experiments, we implement the corrections inside GRPO [22], which forms group-normalized advantages and then applies a PPO-style clipped surrogate with an explicit KL penalty. More connection and implementation details are included in Appendix A and B.

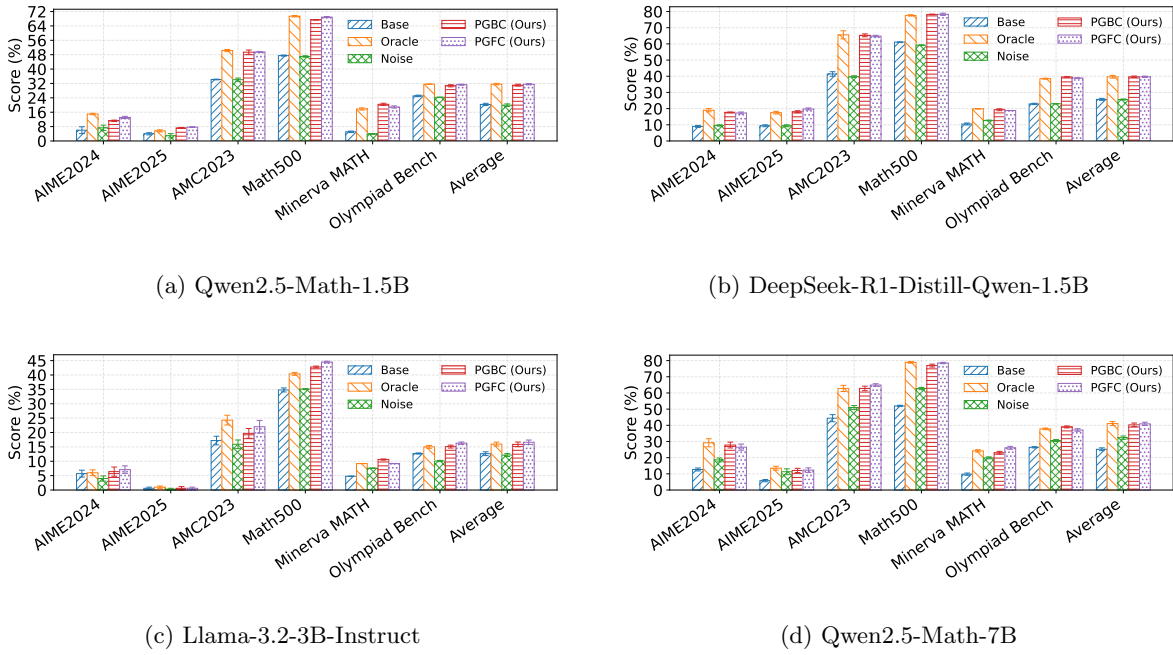


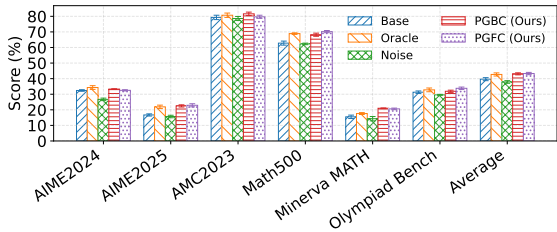
Figure 2: Synthetic-Noise Results (**pass@1**) with 16 samples and 5 random seeds on the four backbones. **Base**: baseline without RL; **Oracle**: Training with clean rewards; **Noise**: Training with noisy verifier rewards; **Noise BC**: Training with noise under backward correction; **Noise FC**: Training with noise under forward correction.

4. Experiments

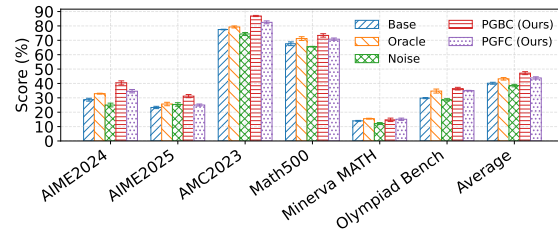
We evaluate our approach under both *synthetic* and *real-world* verifier noise. We first spell out the experimental protocol, and then present main and ablation results.

4.1. Experimental Setup

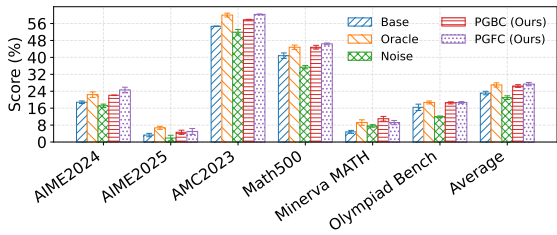
We train on three small backbones, *Qwen2.5-Math-1.5B*, *DeepSeek-R1-Distill-Qwen-1.5B*, and *Llama-3.2-3B-Instruct*, and probe scale with *Qwen2.5-Math-7B*. Rewards come from either (i) a rule-based checker that extracts the final `\boxed{\cdot}` answer and tests numeric/rational equivalence or (ii) a lightweight LLM verifier (**TinyV 1.5B**) used for appeals/estimation; prior work motivates explicit noise modeling due to systematic FP/FN behavior in these verifiers. Unless stated otherwise, we follow the **DeepScaleR** corpus and a GRPO-style on-policy recipe with BoN sampling, implementing our *backward* and *forward* corrections as drop-in hooks at the



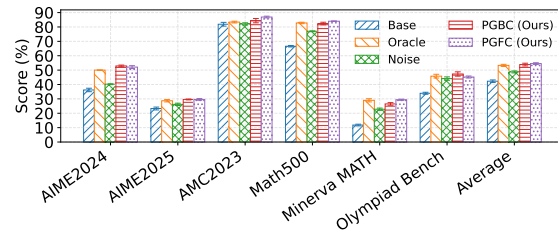
(a) Qwen2.5-Math-1.5B



(b) DeepSeek-R1-Distill-Qwen-1.5B



(c) Llama-3.2-3B-Instruct



(d) Qwen2.5-Math-7B

Figure 3: Synthetic-Noise Results (**pass@8**) with 16 samples and 5 random seeds on the four backbones *Llama-3.2-3B-Instruct*, and *Qwen2.5-Math-7B*. **Base**: baseline without RL; **Oracle**: Training with clean rewards; **Noise**: Training with noisy verifier rewards; **Noise BC**: Training with noise under backward correction; **Noise FC**: Training with noise under forward correction. advantage-construction stage within VERL. Evaluation uses six verifiable math suites—AIME-2024, AIME-2025, AMC-2023, MATH500, MINERVA MATH, and OLYMPIADBENCH—reporting *Pass@1* and *Pass@8* with 16 samples and 5 random seeds in average. Compute is $8 \times$ A100 (40GB) GPUs servers; unless noted, KL schedules, sampling temperatures, and other rollout settings are kept identical across compared conditions. More details can be found in Appendix D.

4.2. Synthetic Noise

To disentangle optimization effects from verifier unreliability, we inject *verifier-conditional* noise into the binary reward stream during training. Concretely, when the latent clean reward is $R^* \in \{0, 1\}$, the observed reward \tilde{R} is drawn from a reward channel with $\Pr(\tilde{R}=1 | R^*=0) = \rho_0$ and $\Pr(\tilde{R}=0 | R^*=1) = \rho_1$; unless stated otherwise we use $\rho_0=0.1$ and $\rho_1=0.2$. We train GRPO on DeepScaleR with identical sampling and KL settings across conditions, and evaluate Pass@1 (16 samples) and Pass@8 on AIME-2024/2025, AMC-2023, MATH500, MINERVA MATH, and OLYMPIADBENCH. We compare five variants: *Base* (no RL), *Oracle* (clean rewards), *Noise*

(uncorrected), and our two corrections—*PGBC* (backward correction using $\hat{R} = \frac{\tilde{R} - \rho_0}{1 - \rho_0 - \rho_1}$) and *PGFC* (forward correction that rescales the gradient using ρ_1 only).

As illustrated in Figure 2 and Figure 3, across models and benchmarks, the injected noise degrades uncorrected GRPO substantially, while both corrections recover most of the gap to the oracle. On *DeepSeek-R1-Distill-Qwen-1.5B*, uncorrected training under noise underperforms the oracle across all tasks (e.g., a noticeably lower Average), whereas *PGBC* and *PGFC* nearly match oracle performance; *PGFC* is consistently as good as or slightly better than *PGBC*, echoing its variance advantages from avoiding division by $(1 - \rho_0 - \rho_1)$. From *Qwen2.5-Math-1.5B* and *DeepSeek-R1-Distill-Qwen-1.5B*, as well as the up-scale model *Qwen2.5-Math-7B*, we observe the same pattern: noise hurts, *PGBC/PGFC* close the gap compared with *Oracle*.

4.3. Real-World Noise

As discussed above, automated verifiers exhibit both *false positives* (LLM judges over-crediting incorrect solutions) and *false negatives* (rule-based checkers rejecting correct ones) [3, 33, 6, 14]. In math RL pipelines, the latter is particularly prevalent: brittle exact-match or limited equivalence rules lead to many valid answers being scored as incorrect, depriving the agent of learning signal. Motivated by this, in this subsection we specifically investigate whether denoising *false negatives*—i.e., estimating $\hat{\rho}_1$ as in Section 3.3—can measurably improve policy optimization. Concretely, we keep a fast rule-based checker as the *primary* reward source and, whenever it returns $\tilde{R}=0$, trigger an *appeals* pass with a lightweight LLM verifier (TinyV) [33]. From disagreements on negatives we maintain an online estimate $\hat{\rho}_1$ (EMA over a sliding window to track policy drift).

Results in Table 1 and Table 2 show a consistent pattern across backbones and benchmarks. Using a LLM *as the reward* (LV) underperforms the rule-based pipeline, corroborating prior observations that LLM judges are bias-prone and gameable [3, 24]. Employing the LLM *as adds-on* to recheck rule-based negatives (**Adds on**) reduces FN and yields a modest but reliable lift, yet the benefit remains indirect because the primary gradient is still driven by noisy binary rewards. In contrast, our *forward correction* (FC0) directly applies the FN correction to the policy gradient via weights $w_{\tilde{R}} \in \{\hat{\rho}_1 - 1, \hat{\rho}_1\}$, and it delivers the strongest and stable improvements.

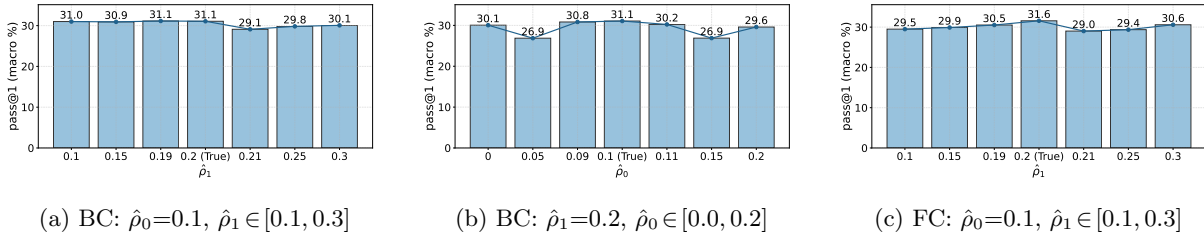


Figure 4: Robustness results. (a) Backward correction (BC) with $\hat{\rho}_0$ fixed and sweeping $\hat{\rho}_1$; (b) Backward correction (BC) with $\hat{\rho}_1$ fixed and sweeping $\hat{\rho}_0$; (c) Forward correction (FC) with $\hat{\rho}_0$ fixed and sweeping $\hat{\rho}_1$.

4.4. Robustness to Noise Mis-Specification

There now exist practical procedures to *estimate* verifier FP/FN rates via rule-based equivalence checkers (e.g., MATH-VERIFY), lightweight appeals/judges such as TinyV, and meta-evaluation suites that quantify verifier reliability [7, 33, 14]. In real deployments, however, these estimates can be imperfect. We therefore test how *backward* and *forward* corrections behave under mis-specified noise rates. We follow the synthetic-noise setting from Section 4.2 with Qwen2.5-math-1.5B: rewards are *corrupted at data-time* with $\rho_0=0.1$, $\rho_1=0.2$. During training, we *intentionally* feed each algorithm mis-specified rates from a grid $\hat{\rho}_0 \in [0.0, 0.2]$, $\hat{\rho}_1 \in [0.1, 0.3]$, and report the Average Pass@1 (16 samples) across our six benchmarks. Because the forward method only requires the false negative rate, we vary $\hat{\rho}_1$ for forward correction while keeping $\hat{\rho}_0$ unused, as shown in Fig. 4.

Backward correction remains strong when the total noise is underestimated, but performance degrades as we overestimate the rates (i.e., as $1 - \hat{\rho}_0 - \hat{\rho}_1$ shrinks). Intuitively, the unbiased de-biasing, $\hat{R} = \frac{\tilde{R} - \hat{\rho}_0}{1 - \hat{\rho}_0 - \hat{\rho}_1}$, involves an inverse factor that amplifies reward variance and accentuates estimation error when the effective denominator becomes small. In contrast, *forward* correction exhibits a notably flat response curve around the true ρ_1 ; perturbing $\hat{\rho}_1$ changes only the per-sample weights and avoids any inverse operation, yielding lower-variance policy gradient estimates.

4.5. Case Studies

We also provide typical failure modes observed during math RL with automated verifiers on Qwen2.5-Math-7B under MATH500 dataset. For rule-based verifier: 52 FNs and 0 FP out of 500

items (marginal rates 10.4% and 0%); for LLM verifier: 81 FNs and 168 FPs out of 500 items (marginal rates 16.2% and 33.6%). The FP case shows an LLM judge over-crediting a malformed solution, while the FN case shows a rule-based checker rejecting a numerically correct answer due to formatting. The raw context can be found in Appendix E.

False Positive (FP).

Problem. Compute: $1 - 2 + 3 - 4 + \dots + 99 - 100$.

Ground truth. $\boxed{-50}$

Model response (excerpt).

Compute: $\$1+2-3-4+5+6-7-8+\backslash dots+97+98-99-100\$.$

$\backslash boxed{ } \backslash boxed{ } \backslash boxed{ } \backslash dots$

Verifier signals. Rule-based checker: X (incorrect); LLM judge: \checkmark (incorrectly accepts) $\Rightarrow \text{FP}$.

False Negative (FN).

Problem. Each of seven islands independently has treasure with probability $\frac{1}{5}$. What is the probability that exactly four islands have treasure?

Correct answer. $\boxed{\frac{448}{15625}}$ (equals 0.028672).

Model answer. $\boxed{0.028672}$

Verifier signals. Rule-based exact-match: X (expects a fraction); numeric equivalence check: \checkmark (values match) $\Rightarrow \text{FN}$.

5. Conclusion

Reinforcement Learning with Verifiable Rewards (RLVR) has emerged as a practical and popular paradigm for training reasoning-focused large language models (LLMs). Yet binarized rewards inevitably suffer from *false positives* (FP) and *false negatives* (FN). Prior efforts largely mitigated these errors from the verifier side—e.g., debiasing LLM judges or strengthening equivalence checking—to reduce the downstream impact on learning [14, 6]. In contrast, we modeled verifier unreliability as a verifier-conditional noise channel with the FP and FN rates, and introduced two

theory-driven corrections that act directly at the policy-learning interface. The *backward* correction de-biases the observed reward to yield an unbiased gradient estimator; it requires estimates the FP and FN rates but is agnostic to the choice of policy-optimization algorithm and can thus be used beyond policy gradient methods. The *forward* correction rescales score-function terms so that the expected update is aligned with the clean gradient; notably, it needs only the FN rate estimate, which is often the dominant source of real-world noise due to rule-based FNs [6, 33].

While we instantiated appeals with a lightweight LLM verifier for efficiency, the same backward/-forward correction mechanisms should also gain from stronger verifiers [33]. Meanwhile, currently using the constant noise rate, the proposed methods already show clear advantages. This means that the constant noise rates approximate the real-world noise rates quite well. However, real-world noise can be very complex, e.g., depending both on the contents and verifiers, leaving interesting future directions.

References

- [1] Guiming Hardy Chen, Shunian Chen, Ziche Liu, Feng Jiang, and Benyou Wang. Humans or llms as the judge? a study on judgement bias. In *Proceedings of the 2024 Conference on Empirical Methods in Natural Language Processing*, pp. 8301–8327, 2024.
- [2] Karl Cobbe, Vineet Kosaraju, Mohammad Bavarian, Mark Chen, Heewoo Jun, Lukasz Kaiser, Matthias Plappert, Jerry Tworek, Jacob Hilton, Reiichiro Nakano, Christopher Hesse, and John Schulman. Training verifiers to solve math word problems. *arXiv preprint arXiv:2110.14168*, 2021.
- [3] Jiawei Gu, Xuhui Jiang, Zhichao Shi, Hexiang Tan, Xuehao Zhai, Chengjin Xu, Wei Li, Yinghan Shen, Shengjie Ma, Honghao Liu, Saizhuo Wang, Kun Zhang, Yuanzhuo Wang, Wen Gao, Lionel Ni, and Jian Guo. A survey on llm-as-a-judge. *arXiv preprint arXiv:2411.15594*, 2024.
- [4] Bo Han, Quanming Yao, Xingrui Yu, Gang Niu, Miao Xu, Weihua Hu, Ivor W. Tsang, and Masashi Sugiyama. Co-teaching: Robust training of deep neural networks with extremely noisy labels. In Samy Bengio, Hanna M. Wallach, Hugo Larochelle, Kristen Grauman, Nicolò Cesa-Bianchi, and Roman Garnett (eds.), *Advances in Neural Information Processing*

Systems 31: Annual Conference on Neural Information Processing Systems 2018, NeurIPS 2018, December 3-8, 2018, Montréal, Canada, pp. 8536–8546, 2018.

- [5] Chaoqun He, Renjie Luo, Yuzhuo Bai, Shengding Hu, Zhen Leng Thai, Junhao Shen, Jinyi Hu, Xu Han, Yujie Huang, Yuxiang Zhang, Jie Liu, Lei Qi, Zhiyuan Liu, and Maosong Sun. Olympiadbench: A challenging benchmark for promoting AGI with olympiad-level bilingual multimodal scientific problems. In Lun-Wei Ku, Andre Martins, and Vivek Srikumar (eds.), *Proceedings of the 62nd Annual Meeting of the Association for Computational Linguistics (Volume 1: Long Papers), ACL 2024, Bangkok, Thailand, August 11-16, 2024*, pp. 3828–3850. Association for Computational Linguistics, 2024.
- [6] Yuzhen Huang, Weihao Zeng, Xingshan Zeng, Qi Zhu, and Junxian He. Pitfalls of rule- and model-based verifiers—a case study on mathematical reasoning. *arXiv preprint arXiv:2505.22203*, 2025.
- [7] Hugging Face. Math-verify: A robust mathematical expression evaluator for llm outputs. GitHub repository, 2025. URL <https://github.com/huggingface/Math-Verify>.
- [8] HuggingFaceH4. Aime 2024 (dataset card). Hugging Face, 2024. URL https://huggingface.co/datasets/HuggingFaceH4/aime_2024.
- [9] Lu Jiang, Zhengyuan Zhou, Thomas Leung, Li-Jia Li, and Li Fei-Fei. Mentornet: Learning data-driven curriculum for very deep neural networks on corrupted labels. In Jennifer G. Dy and Andreas Krause (eds.), *Proceedings of the 35th International Conference on Machine Learning, ICML 2018, Stockholmsmässan, Stockholm, Sweden, July 10-15, 2018*, volume 80 of *Proceedings of Machine Learning Research*, pp. 2309–2318. PMLR, 2018.
- [10] Vishesh Karwa and Edoardo M Aioldi. On the admissibility of horvitz-thompson estimator for estimating causal effects under network interference. *arXiv preprint arXiv:2312.01234*, 2023.
- [11] Aitor Lewkowycz, Anders Andreassen, David Dohan, Ethan Dyer, Henryk Michalewski, Vinay V. Ramasesh, Ambrose Slone, Cem Anil, Imanol Schlag, Theo Gutman-Solo, Yuhuai Wu, Behnam Neyshabur, Guy Gur-Ari, and Vedant Misra. Solving quantitative reasoning problems with language models. In Sanmi Koyejo, S. Mohamed, A. Agarwal, Danielle Belgrave, K. Cho, and A. Oh (eds.), *Advances in Neural Information Processing Systems 35:*

Annual Conference on Neural Information Processing Systems 2022, NeurIPS 2022, New Orleans, LA, USA, November 28 - December 9, 2022.

- [12] Junnan Li, Richard Socher, and Steven C. H. Hoi. Dividemix: Learning with noisy labels as semi-supervised learning. In *8th International Conference on Learning Representations, ICLR 2020, Addis Ababa, Ethiopia, April 26-30, 2020*. OpenReview.net, 2020.
- [13] Xuefeng Li, Tongliang Liu, Bo Han, Gang Niu, and Masashi Sugiyama. Provably end-to-end label-noise learning without anchor points. In Marina Meila and Tong Zhang (eds.), *Proceedings of the 38th International Conference on Machine Learning, ICML 2021, 18-24 July 2021, Virtual Event*, volume 139 of *Proceedings of Machine Learning Research*, pp. 6403–6413. PMLR, 2021.
- [14] Xuzhao Li, Xuchen Li, Shiyu Hu, Yongzhen Guo, and Wentao Zhang. Verifybench: A systematic benchmark for evaluating reasoning verifiers across domains. *arXiv preprint arXiv:2507.09884*, 2025.
- [15] Hunter Lightman, Vineet Kosaraju, Yuri Burda, Harrison Edwards, Bowen Baker, Teddy Lee, Jan Leike, John Schulman, Ilya Sutskever, and Karl Cobbe. Let’s verify step by step. In *The Twelfth International Conference on Learning Representations, ICLR 2024, Vienna, Austria, May 7-11, 2024*. OpenReview.net, 2024.
- [16] Michael Luo, Sijun Tan, Justin Wong, Xiaoxiang Shi, William Y. Tang, Manan Roongta, Colin Cai, Jeffrey Luo, Li Erran Li, Raluca Ada Popa, and Ion Stoica. Deepscaler: Surpassing o1-preview with a 1.5b model by scaling rl. <https://pretty-radio-b75.notion.site/DeepScaleR-Surpassing-01-Preview-with-a-1-5B-Model-by-Scaling-RL-19681902c1468005bed8ca30> 2025. Notion Blog.
- [17] math-ai. Amc 2023 (dataset card). Hugging Face, 2025. URL <https://huggingface.co/datasets/math-ai/amc23>.
- [18] Youssef Mroueh. Reinforcement learning with verifiable rewards: Grpo’s effective loss, dynamics, and success amplification. *arXiv preprint arXiv:2503.06639*, 2025.
- [19] Nagarajan Natarajan, Inderjit S. Dhillon, Pradeep Ravikumar, and Ambuj Tewari. Learning with noisy labels. In Christopher J. C. Burges, Léon Bottou, Zoubin Ghahramani,

and Kilian Q. Weinberger (eds.), *Advances in Neural Information Processing Systems 26: 27th Annual Conference on Neural Information Processing Systems 2013. Proceedings of a meeting held December 5-8, 2013, Lake Tahoe, Nevada, United States*, pp. 1196–1204, 2013.

[20] OpenCompass. Aime 2025 (dataset card). Hugging Face, 2025. URL <https://huggingface.co/datasets/opencompass/AIME2025>.

[21] Giorgio Patrini, Alessandro Rozza, Aditya Krishna Menon, Richard Nock, and Lizhen Qu. Making deep neural networks robust to label noise: A loss correction approach. In *2017 IEEE Conference on Computer Vision and Pattern Recognition, CVPR 2017, Honolulu, HI, USA, July 21-26, 2017*, pp. 2233–2241. IEEE Computer Society, 2017.

[22] Zhihong Shao, Peiyi Wang, Qihao Zhu, Runxin Xu, Junxiao Song, Mingchuan Zhang, Y. K. Li, Y. Wu, and Daya Guo. Deepseekmath: Pushing the limits of mathematical reasoning in open language models. *arXiv preprint arXiv:2402.03300*, 2024.

[23] Jiawen Shi, Zenghui Yuan, Yinuo Liu, Yue Huang, Pan Zhou, Lichao Sun, and Neil Zhenqiang Gong. Optimization-based prompt injection attack to llm-as-a-judge. In Bo Luo, Xiaojing Liao, Jun Xu, Engin Kirda, and David Lie (eds.), *Proceedings of the 2024 on ACM SIGSAC Conference on Computer and Communications Security, CCS 2024, Salt Lake City, UT, USA, October 14-18, 2024*, pp. 660–674. ACM, 2024.

[24] Lin Shi, Chiyu Ma, Wenhua Liang, Xingjian Diao, Weicheng Ma, and Soroush Vosoughi. Judging the judges: A systematic study of position bias in llm-as-a-judge. *arXiv preprint arXiv:2406.07791*, 2025.

[25] Hwanjun Song, Minseok Kim, Dongmin Park, Yooju Shin, and Jae-Gil Lee. Learning from noisy labels with deep neural networks: A survey. *IEEE transactions on neural networks and learning systems*, 34(11):8135–8153, 2022.

[26] Richard S. Sutton, David A. McAllester, Satinder Singh, and Yishay Mansour. Policy gradient methods for reinforcement learning with function approximation. In Sara A. Solla, Todd K. Leen, and Klaus-Robert Müller (eds.), *Advances in Neural Information Processing Systems 12, [NIPS Conference, Denver, Colorado, USA, November 29 - December 4, 1999]*, pp. 1057–1063. The MIT Press, 1999.

[27] Aman Singh Thakur, Kartik Choudhary, Venkat Srinik Ramayapally, Sankaran Vaidyanathan, and Dieuwke Hupkes. Judging the judges: Evaluating alignment and vulnerabilities in llms-as-judges. *arXiv preprint arXiv:2406.12624*, 2024.

[28] Jingkang Wang, Yang Liu, and Bo Li. Reinforcement learning with perturbed rewards. In *The Thirty-Fourth AAAI Conference on Artificial Intelligence, AAAI 2020, The Thirty-Second Innovative Applications of Artificial Intelligence Conference, IAAI 2020, The Tenth AAAI Symposium on Educational Advances in Artificial Intelligence, EAAI 2020, New York, NY, USA, February 7-12, 2020*, pp. 6202–6209. AAAI Press, 2020.

[29] Xuezhi Wang, Jason Wei, Dale Schuurmans, Quoc V. Le, Ed H. Chi, Sharan Narang, Aakanksha Chowdhery, and Denny Zhou. Self-consistency improves chain of thought reasoning in language models. In *The Eleventh International Conference on Learning Representations, ICLR 2023, Kigali, Rwanda, May 1-5, 2023*. OpenReview.net, 2023.

[30] Jason Wei, Xuezhi Wang, Dale Schuurmans, Maarten Bosma, Brian Ichter, Fei Xia, Ed H. Chi, Quoc V. Le, and Denny Zhou. Chain-of-thought prompting elicits reasoning in large language models. In Sanmi Koyejo, S. Mohamed, A. Agarwal, Danielle Belgrave, K. Cho, and A. Oh (eds.), *Advances in Neural Information Processing Systems 35: Annual Conference on Neural Information Processing Systems 2022, NeurIPS 2022, New Orleans, LA, USA, November 28 - December 9, 2022*.

[31] Xumeng Wen, Zihan Liu, Shun Zheng, Zhijian Xu, Shengyu Ye, Zhirong Wu, Xiao Liang, Yang Wang, Junjie Li, Ziming Miao, Jiang Bian, and Mao Yang. Reinforcement learning with verifiable rewards implicitly incentivizes correct reasoning in base llms. *arXiv preprint arXiv:2506.14245*, 2025.

[32] Ronald J Williams. Simple statistical gradient-following algorithms for connectionist reinforcement learning. *Machine Learning*, 8(3):229–256, 1992.

[33] Zhangchen Xu, Yuetai Li, Fengqing Jiang, Bhaskar Ramasubramanian, Luyao Niu, Bill Yuchen Lin, and Radha Poovendran. Tinyv: Reducing false negatives in verification improves rl for llm reasoning. *arXiv preprint arXiv:2505.14625*, 2025.

[34] Shunyu Yao, Dian Yu, Jeffrey Zhao, Izhak Shafran, Tom Griffiths, Yuan Cao, and Karthik Narasimhan. Tree of thoughts: Deliberate problem solving with large language models.

In Alice Oh, Tristan Naumann, Amir Globerson, Kate Saenko, Moritz Hardt, and Sergey Levine (eds.), *Advances in Neural Information Processing Systems 36: Annual Conference on Neural Information Processing Systems 2023, NeurIPS 2023, New Orleans, LA, USA, December 10 - 16, 2023*.

- [35] Yulai Zhao, Haolin Liu, Dian Yu, SY Kung, Haitao Mi, and Dong Yu. One token to fool llm-as-a-judge. *arXiv preprint arXiv:2507.08794*, 2025.
- [36] Denny Zhou, Nathanael Schärli, Le Hou, Jason Wei, Nathan Scales, Xuezhi Wang, Dale Schuurmans, Claire Cui, Olivier Bousquet, Quoc V. Le, and Ed H. Chi. Least-to-most prompting enables complex reasoning in large language models. In *The Eleventh International Conference on Learning Representations, ICLR 2023, Kigali, Rwanda, May 1-5, 2023*. OpenReview.net, 2023.

A. From REINFORCE-Style Corrections to GRPO Updates

Setup (single prompt and group). Fix a prompt x and sample a group of K i.i.d. responses $y_1, \dots, y_K \sim \pi_\theta(\cdot \mid x)$. Let $G_i \triangleq \sum_{t=1}^{|y_i|} \nabla_\theta \log \pi_\theta(y_{i,t} \mid x, y_{i,<t})$ denote the trajectory score-function. Let u_i be any scalar *proxy reward* computed from the trajectory (e.g., $u_i = \hat{r}_i$ for PGBC, or $u_i = w_{\tilde{r}_i}$ for PGFC), and define the group mean $\bar{u} = \frac{1}{K} \sum_{j=1}^K u_j$. Consider the centered score-function update

$$\Delta_{\text{center}}(\theta) \triangleq \frac{1}{K} \sum_{i=1}^K (u_i - \bar{u}) G_i. \quad (4)$$

Proposition 3 (Group centering preserves expected direction). *Assume $\{(u_i, G_i)\}_{i=1}^K$ are i.i.d. under $\pi_\theta(\cdot \mid x)$ and $\mathbb{E}[G_i \mid x] = 0$ (the standard score-function identity [32, 26]). Then the centered update in (4) satisfies*

$$\mathbb{E}[\Delta_{\text{center}}(\theta) \mid x] = \left(1 - \frac{1}{K}\right) \mathbb{E}[u G \mid x]. \quad (5)$$

In particular, if $\mathbb{E}[u G \mid x]$ is parallel to the clean gradient direction for the prompt-conditioned objective, then so is $\mathbb{E}[\Delta_{\text{center}}(\theta) \mid x]$.

Proof. Expand $\Delta_{\text{center}} = \frac{1}{K} \sum_i u_i G_i - \bar{u} \cdot \frac{1}{K} \sum_i G_i$. Taking expectation conditioned on x yields

$$\mathbb{E}[\bar{u} \cdot \frac{1}{K} \sum_i G_i \mid x] = \frac{1}{K^2} \sum_{i,j} \mathbb{E}[u_j G_i \mid x].$$

The $i = j$ terms contribute $\frac{K}{K^2} \mathbb{E}[u G \mid x]$. For $i \neq j$, independence gives $\mathbb{E}[u_j G_i \mid x] = \mathbb{E}[u \mid x] \mathbb{E}[G \mid x] = 0$. Thus $\mathbb{E}[\bar{u} \cdot \frac{1}{K} \sum_i G_i \mid x] = \frac{1}{K} \mathbb{E}[u G \mid x]$, implying (5). \square

Corollary 1 (Directional correctness of PGFC under centered GRPO-style updates). Under the Verifier Reward Channel (Definition 1) and the conditional-independence assumption stated above, let $u = w_{\tilde{R}}$ with $w_0 = \rho_1 - 1$ and $w_1 = \rho_1$ as in Proposition 2. Then for each prompt x ,

$$\mathbb{E}[\Delta_{\text{center}}(\theta) \mid x] = \left(1 - \frac{1}{K}\right) (1 - \rho_0 - \rho_1) \nabla_\theta J(\theta \mid x),$$

so the expected centered update remains aligned with the clean policy-gradient direction.

Standardization, clipping, and KL (what is guaranteed, and what is approximate). GRPO further divides centered proxy rewards by the within-group standard deviation to form normalized advantages, and then applies a PPO-style clipping on token-level ratios and an explicit KL penalty to π_{ref} [22]. The exact direction-preservation statement in Proposition 3 covers the *centering* step, which is the main nontrivial departure from vanilla REINFORCE. The additional standardization is a multiplication by a random positive scalar; this primarily acts as an adaptive step-size (and cannot flip the sign of individual sample advantages), though a strict equality in expectation would require additional concentration assumptions. Clipping and the KL penalty add further stabilizers: in the small-update regime (encouraged by the KL term and typical learning rates), clipping is rarely active and the update is close to the unclipped score-function form; when clipping activates, it intentionally limits step size and may deviate from the exact REINFORCE direction. Importantly, our corrections target the *reward-gradient component*; the KL gradient is unchanged, so any global scaling factor (e.g., $1 - \rho_0 - \rho_1$) can be absorbed into the effective learning rate and/or interpreted as modifying the reward–KL trade-off.

B. Implementation Details

We describe how to integrate Algorithm 1 (backward, unbiased reward de-biasing) and Algorithm 2 (forward, gradient-scaled) into *Group Relative Policy Optimization* (GRPO) under both *outcome* and *process* supervision. GRPO samples, for each prompt x , a group of K responses $\{y_i\}_{i=1}^K$ from the behavior policy, computes a *group-normalized advantage* for each sample (or step), and then applies a PPO-style clipped surrogate with a separate KL regularizer to a reference policy; no value network is used. Our modifications are confined to the advantage-construction stage, leaving ratio clipping and KL loss unchanged (details of GRPO in [22] and open-source implementations).

Notation (shared). Let π_θ be the current policy and π_{old} the behavior policy. Define token-level ratios $r_{i,t} = \frac{\pi_\theta(y_{i,t}|x, y_{i,<t})}{\pi_{\text{old}}(y_{i,t}|x, y_{i,<t})}$. GRPO’s PPO-style surrogate at token t uses an advantage $A_{i,t}$:

$$\mathcal{L}_{\text{grpo}}(\theta) = \frac{1}{K} \sum_{i=1}^K \frac{1}{|y_i|} \sum_{t=1}^{|y_i|} \min(r_{i,t} A_{i,t}, \text{clip}(r_{i,t}, 1 \pm \varepsilon) A_{i,t}) - \beta \text{KL}(\pi_\theta \| \pi_{\text{ref}}),$$

where the KL term is added to the loss rather than folded into the reward. Our corrections only change how $A_{i,t}$ is formed.

Outcome Supervision (one scalar reward per response)

For each i , we observe a binary verifier reward $\tilde{r}_i \in \{0, 1\}$.

Algo 1 (Backward) in GRPO. First construct an *unbiased* per-sample reward

$$\hat{r}_i = \frac{\tilde{r}_i - \hat{\rho}_0}{1 - \hat{\rho}_0 - \hat{\rho}_1}.$$

Compute group statistics on $\{\hat{r}_i\}_{i=1}^K$:

$$\bar{r} = \frac{1}{K} \sum_{i=1}^K \hat{r}_i, \quad s = \sqrt{\frac{1}{K} \sum_{i=1}^K (\hat{r}_i - \bar{r})^2}.$$

Define the group-normalized advantage *constant across tokens* of the same response,

$$a_i^{(\text{back})} = \frac{\hat{r}_i - \bar{r}}{s + \varepsilon}, \quad A_{i,t} \equiv a_i^{(\text{back})}, \quad \forall t.$$

This is a drop-in replacement for the usual GRPO outcome-advantage, with the sole change being that the group mean/variance are computed over de-noised rewards \hat{r}_i rather than raw \tilde{r}_i .

Algo 2 (Forward) in GRPO (Pre-Center). To ensure the gradient direction aligns with Theorem 2, we adopt a *pre-center* approach where the correction weights are treated as proxy rewards before normalization. First, define the forward weight for each trajectory based on the observed reward \tilde{r}_i and the estimated false negative rate $\hat{\rho}_1$:

$$w_i = \begin{cases} \hat{\rho}_1 - 1, & \text{if } \tilde{r}_i = 0, \\ \hat{\rho}_1, & \text{if } \tilde{r}_i = 1. \end{cases}$$

We use these weights directly as the proxy rewards for the GRPO advantage calculation:

$$\mathcal{R}_i^{\text{proxy}} = w_i.$$

Then, apply standard GRPO group normalization to these proxy rewards:

$$a_i^{(\text{fwd})} = \frac{\mathcal{R}_i^{\text{proxy}} - \overline{\mathcal{R}^{\text{proxy}}}}{\text{std}(\{\mathcal{R}_j^{\text{proxy}}\}) + \varepsilon}, \quad A_{i,t} \equiv a_i^{(\text{fwd})}, \quad \forall t.$$

This pre-centering ensures that negative samples (where $w_i < 0$) are correctly positioned relative to the group mean, preserving the sign logic required to suppress false negatives without inadvertently flipping the optimization direction.

Post-Center Option. Alternatively, one could apply the weights *after* calculating the standard advantages (*post-center*):

$$A_{i,t}^{(\text{post})} \leftarrow w_i \cdot \left(\frac{\tilde{r}_i - \bar{\tilde{r}}}{\text{std}(\{\tilde{r}_j\}) + \varepsilon} \right).$$

However, we note that if w_i is negative (e.g., $\hat{\rho}_1 - 1$ for $\tilde{r}_i = 0$), multiplying it by a typically negative advantage (for $\tilde{r}_i = 0$) would flip the sign to positive, potentially encouraging incorrect behaviors. Our default implementation and reported results therefore use the **pre-center** formulation, which is theoretically consistent with our derivation. We provide the post-center variant solely as an engineering option in our code.

Process Supervision (step-wise rewards)

Suppose each response y_i has step indices $\text{index}_i(1) < \dots < \text{index}_i(K_i)$ with step-level observed rewards $\tilde{r}_i^{(j)}$ attached at those indices.

Algo 1 (Backward) in GRPO-Process. De-noise each step reward:

$$\hat{r}_i^{(j)} = \frac{\tilde{r}_i^{(j)} - \hat{\rho}_0}{1 - \hat{\rho}_0 - \hat{\rho}_1}.$$

Normalize across the *group and steps* in the current batch following GRPO's process recipe:

$$\tilde{r}_i^{(j)} = \frac{\hat{r}_i^{(j)} - \text{mean}(\{\hat{r}_\ell^{(m)}\})}{\text{std}(\{\hat{r}_\ell^{(m)}\}) + \varepsilon}.$$

Accumulate into token-level advantages (for all tokens t at or before the j -th step boundary):

$$A_{i,t} = \sum_{\text{index}_i(j) \geq t} \tilde{r}_i^{(j)}.$$

Algo 2 (Forward) in GRPO-Process (Pre-Center). Similar to the outcome case, we apply weights directly to the step-level rewards before normalization. Define the step-level weights:

$$w_i^{(j)} = \begin{cases} \hat{\rho}_1 - 1, & \text{if } \tilde{r}_i^{(j)} = 0, \\ \hat{\rho}_1, & \text{if } \tilde{r}_i^{(j)} = 1. \end{cases}$$

Use these as proxy rewards $\mathcal{R}_i^{(j),\text{proxy}} = w_i^{(j)}$, normalize them across the group and steps to obtain $\tilde{r}_i^{(j)}$, and finally accumulate the token advantages:

$$A_{i,t} = \sum_{\text{index}_i(j) \geq t} \tilde{r}_i^{(j)}.$$

Scope of verifier-noise regimes. While both FPs and FNs appear in practice, many math-RL pipelines rely on rule-based or programmatic checkers whose FP rate is typically negligible but whose FN rate can be substantial due to brittleness (formatting, algebraic equivalence, or answer representation). Our real-world experiments therefore emphasize this *FN-dominant* regime and evaluate whether explicitly correcting the policy update using an online estimate of ρ_1 improves learning beyond simply rechecking negatives. In contrast, LLM-as-a-judge regimes can exhibit higher and non-stationary FP rates and may violate instance-independence more severely; we discuss the implications and recommended usage of PGBC/PGFC across regimes in Table 3.

When conditional independence is violated (bias decomposition). Our directional-alignment results rely on conditional independence to factorize $\mathbb{E}[w_{\tilde{R}}G \mid R^*] = \mathbb{E}[w_{\tilde{R}} \mid R^*]\mathbb{E}[G \mid R^*]$. If verifier errors depend on trajectory features beyond correctness (e.g., style-based FP hacks), the update admits the decomposition

$$\mathbb{E}[w_{\tilde{R}}G \mid R^*] = \mathbb{E}[w_{\tilde{R}} \mid R^*]\mathbb{E}[G \mid R^*] + \text{Cov}(w_{\tilde{R}}, G \mid R^*),$$

so the residual bias is governed by the conditional covariance term. This highlights a practical diagnostic: if verifier decisions are strongly predictable from superficial cues that also affect generation likelihood, $\text{Cov}(w_{\tilde{R}}, G \mid R^*)$ may be non-negligible and one should combine channel-based correction with verifier hardening or instance-dependent reliability modeling.

Online FN-rate estimation via appeals implementation details. At training step t , let $\mathcal{N}_R^{(t)}$ denote trajectories labeled negative by the rule-based verifier and $\mathcal{P}_R^{(t)}$ denote those labeled positive. We appeal a uniformly random subset $S^{(t)} \subseteq \mathcal{N}_R^{(t)}$ by including each element independently with probability $q \in (0, 1]$ and re-evaluating it using a lightweight LLM verifier (TinyV [33]). Let $\mathcal{P}_L^{(t)} \subseteq S^{(t)}$ be the appealed negatives that TinyV flips to positive (i.e., rule-negative & LLM-positive). Using a Horvitz–Thompson correction [10], we estimate the number of false negatives among rule-based negatives by

$$\widehat{\text{FN}}^{(t)} = \frac{|\mathcal{P}_L^{(t)}|}{q},$$

which is unbiased under uniform subsampling. Assuming rule-based positives have negligible FP rate, we treat $|\mathcal{P}_R^{(t)}|$ as a proxy for true positives and estimate the FN rate as

$$\hat{\rho}_1^{(t)} = \frac{\widehat{\text{FN}}^{(t)} + \alpha}{\widehat{\text{FN}}^{(t)} + |\mathcal{P}_R^{(t)}| + \alpha + \beta},$$

with small Beta-prior pseudocounts α, β (we use 10^{-5}) for numerical stability. To track non-stationarity as the policy evolves, we apply exponential moving average (EMA) smoothing,

$$\bar{\rho}_1^{(t)} = \lambda \bar{\rho}_1^{(t-1)} + (1 - \lambda) \hat{\rho}_1^{(t)},$$

and use $\bar{\rho}_1^{(t)}$ as the plug-in estimate in PGFC. The additional verifier cost scales linearly with q : the expected number of TinyV calls per update is $q \cdot |\mathcal{N}_R^{(t)}|$, typically much smaller than the number of rollouts.

High-FP and content-dependent errors (practical guidance). PGFC does not require estimating ρ_0 : under the Verifier Reward Channel model, ρ_0 only affects the positive scaling factor $c = 1 - \rho_0 - \rho_1$ in Theorem 2, which can be absorbed into the effective learning rate. However, if FP patterns are strongly content-dependent (e.g., prompt-hacking phrases for LLM judges), then the channel assumptions may be violated and the covariance term discussed above can bias the update. In such regimes, we recommend treating PGBC/PGFC as complementary to (rather than a replacement for) verifier hardening and hybrid verifier designs (e.g., rule-based checking with appeals, calibrated judges, or adversarially trained verifiers).

C. Proofs and Derivations

C.1. Proof of Proposition 1

Proof. We compute the expectation of the noisy reward \tilde{R} conditioned on the clean reward R^* , which is a binary variable. By the definition of expectation:

$$\begin{aligned} \mathbb{E}[\tilde{R}] &= 1 \cdot \mathbb{P}(\tilde{R} = 1 \mid R^*) + 0 \cdot \mathbb{P}(\tilde{R} = 0 \mid R^*) \\ &= \mathbb{P}(\tilde{R} = 1 \mid R^*). \end{aligned}$$

We can expand this using the law of total probability, conditioning on the value of $R^* \in \{0, 1\}$:

$$\mathbb{E}[\tilde{R} \mid R^*] = R^* \cdot \mathbb{P}(\tilde{R} = 1 \mid R^* = 1) + (1 - R^*) \cdot \mathbb{P}(\tilde{R} = 1 \mid R^* = 0).$$

From Definition 1, we have $\mathbb{P}(\tilde{R} = 1 \mid R^* = 0) = \rho_0$ and $\mathbb{P}(\tilde{R} = 0 \mid R^* = 1) = \rho_1$, which implies $\mathbb{P}(\tilde{R} = 1 \mid R^* = 1) = 1 - \rho_1$. Substituting these values:

$$\begin{aligned}\mathbb{E}[\tilde{R} \mid R^*] &= R^*(1 - \rho_1) + (1 - R^*)\rho_0 \\ &= R^* - \rho_1 R^* + \rho_0 - \rho_0 R^* \\ &= (1 - \rho_0 - \rho_1)R^* + \rho_0.\end{aligned}$$

This completes the proof. \square

C.2. Proof of Theorem 1

Proof. Recall the verifier reward channel (Definition 1): for the latent clean reward $R^* \in \{0, 1\}$ and the observed noisy reward $\tilde{R} \in \{0, 1\}$,

$$\Pr(\tilde{R} = 1 \mid R^* = 0) = \rho_0, \quad \Pr(\tilde{R} = 0 \mid R^* = 1) = \rho_1,$$

hence $\Pr(\tilde{R} = 1 \mid R^* = 1) = 1 - \rho_1$ and $\Pr(\tilde{R} = 0 \mid R^* = 0) = 1 - \rho_0$. Since $1 - \rho_0 - \rho_1 > 0$, the estimator

$$\hat{R} \triangleq \frac{\tilde{R} - \rho_0}{1 - \rho_0 - \rho_1}$$

is well-defined.

We prove unbiasedness by computing the conditional expectation given R^* . First note that because \tilde{R} is binary,

$$\mathbb{E}[\tilde{R} \mid R^*] = 1 \cdot \Pr(\tilde{R} = 1 \mid R^*) + 0 \cdot \Pr(\tilde{R} = 0 \mid R^*) = \Pr(\tilde{R} = 1 \mid R^*). \quad (6)$$

By the channel definition, for the two possible values of R^* we have

$$\mathbb{E}[\tilde{R} \mid R^* = 1] = 1 - \rho_1, \quad \mathbb{E}[\tilde{R} \mid R^* = 0] = \rho_0.$$

These two cases can be written compactly as the affine form (Proposition 1)

$$\mathbb{E}[\tilde{R} \mid R^*] = (1 - \rho_0 - \rho_1)R^* + \rho_0. \quad (7)$$

Now take the conditional expectation of \hat{R} :

$$\begin{aligned}
\mathbb{E}[\hat{R} | R^*] &= \mathbb{E}\left[\frac{\tilde{R} - \rho_0}{1 - \rho_0 - \rho_1} \middle| R^*\right] \\
&= \frac{\mathbb{E}[\tilde{R} | R^*] - \rho_0}{1 - \rho_0 - \rho_1} \\
&= \frac{(1 - \rho_0 - \rho_1)R^* + \rho_0 - \rho_0}{1 - \rho_0 - \rho_1} \quad (\text{by (7)}) \\
&= R^*.
\end{aligned} \tag{8}$$

Equation (8) shows that \hat{R} is an unbiased estimator of the latent clean reward in the conditional sense.

Finally, taking total expectation (law of iterated expectation) yields

$$\mathbb{E}[\hat{R}] = \mathbb{E}[\mathbb{E}[\hat{R} | R^*]] = \mathbb{E}[R^*],$$

so \hat{R} is unbiased for the clean reward both conditionally and unconditionally. \square

C.3. Proof of Proposition 2

Proof. The proposition states two claims about the conditional expectation of the forward weights.

The weights are defined as:

$$w_{\tilde{R}} = \begin{cases} w_0 = \rho_1 - 1 & \text{if } \tilde{R} = 0, \\ w_1 = \rho_1 & \text{if } \tilde{R} = 1. \end{cases}$$

The noise model provides the conditional probabilities:

$$\begin{aligned}
\Pr(\tilde{R} = 0 | R^* = 1) &= \rho_1, & \Pr(\tilde{R} = 1 | R^* = 1) &= 1 - \rho_1 \\
\Pr(\tilde{R} = 1 | R^* = 0) &= \rho_0, & \Pr(\tilde{R} = 0 | R^* = 0) &= 1 - \rho_0
\end{aligned}$$

Part 1: Proof of $\mathbb{E}[w_{\tilde{R}} \mid R^ = 1] = 0$.* We compute the expectation of $w_{\tilde{R}}$ conditioned on the true reward being positive ($R^* = 1$):

$$\begin{aligned}
\mathbb{E}[w_{\tilde{R}} \mid R^* = 1] &= \sum_{k \in \{0,1\}} w_k \cdot \Pr(\tilde{R} = k \mid R^* = 1) \\
&= w_0 \cdot \Pr(\tilde{R} = 0 \mid R^* = 1) + w_1 \cdot \Pr(\tilde{R} = 1 \mid R^* = 1) \\
&= (\rho_1 - 1) \cdot (\rho_1) + (\rho_1) \cdot (1 - \rho_1) \\
&= (\rho_1^2 - \rho_1) + (\rho_1 - \rho_1^2) \\
&= 0.
\end{aligned}$$

Part 2: Proof of $\mathbb{E}[w_{\tilde{R}} \mid R^ = 0] = -(1 - \rho_0 - \rho_1)$.* Next, we compute the expectation of $w_{\tilde{R}}$ conditioned on the true reward being negative ($R^* = 0$):

$$\begin{aligned}
\mathbb{E}[w_{\tilde{R}} \mid R^* = 0] &= \sum_{k \in \{0,1\}} w_k \cdot \Pr(\tilde{R} = k \mid R^* = 0) \\
&= w_0 \cdot \Pr(\tilde{R} = 0 \mid R^* = 0) + w_1 \cdot \Pr(\tilde{R} = 1 \mid R^* = 0) \\
&= (\rho_1 - 1) \cdot (1 - \rho_0) + (\rho_1) \cdot (\rho_0) \\
&= (\rho_1 - \rho_0 \rho_1 - 1 + \rho_0) + \rho_0 \rho_1 \\
&= \rho_1 + \rho_0 - 1 \\
&= -(1 - \rho_0 - \rho_1).
\end{aligned}$$

This proves both claims of the proposition. \square

C.4. Proof of Theorem 2

Proof. We want to show that $\mathbb{E}[\Delta\theta] = (1 - \rho_0 - \rho_1) \nabla_\theta J(\theta)$, where $\Delta\theta = \frac{1}{M} \sum_{t=1}^M h_t$ and $h_t = w_{\tilde{R}} G_t$. By linearity of expectation and assuming i.i.d. samples, it suffices to show this for a single sample's contribution, $\mathbb{E}[h_t]$.

We use the law of total expectation, conditioning on the latent true reward $R^* \in \{0, 1\}$:

$$\begin{aligned}
\mathbb{E}[h_t] &= \mathbb{E}[w_{\tilde{R}} G_t] = \mathbb{E}[\mathbb{E}[w_{\tilde{R}} G_t \mid R^*]] \\
&= \Pr(R^* = 1) \mathbb{E}[w_{\tilde{R}} G_t \mid R^* = 1] + \Pr(R^* = 0) \mathbb{E}[w_{\tilde{R}} G_t \mid R^* = 0].
\end{aligned}$$

The noise process generating \tilde{R} is independent of the policy's action generation process (which produces G_t), conditional on the true reward R^* . Thus, we can separate the expectations:

$$\mathbb{E}[w_{\tilde{R}} G_t \mid R^*] = \mathbb{E}[w_{\tilde{R}} \mid R^*] \cdot \mathbb{E}[G_t \mid R^*].$$

Using the results from Proposition 2:

- $\mathbb{E}[w_{\tilde{R}} \mid R^* = 1] = 0$.
- $\mathbb{E}[w_{\tilde{R}} \mid R^* = 0] = -(1 - \rho_0 - \rho_1)$.

Substituting these back into the main expectation formula:

$$\begin{aligned} \mathbb{E}[w_{\tilde{R}} G_t] &= \Pr(R^* = 1) \cdot (0) \cdot \mathbb{E}[G_t \mid R^* = 1] + \Pr(R^* = 0) \cdot (-(1 - \rho_0 - \rho_1)) \cdot \mathbb{E}[G_t \mid R^* = 0] \\ &= -(1 - \rho_0 - \rho_1) \cdot \Pr(R^* = 0) \mathbb{E}[G_t \mid R^* = 0] \\ &= -(1 - \rho_0 - \rho_1) \cdot \mathbb{E}[\mathbf{1}_{\{R^*=0\}} G_t], \end{aligned}$$

where $\mathbf{1}_{\{\cdot\}}$ is the indicator function. From two fundamental properties of the score function:

1. The unconditional expectation is zero: $\mathbb{E}[G_t] = 0$ [32, 26].
2. The clean policy gradient is $\nabla_{\theta} J(\theta) = \mathbb{E}[R^* G_t]$.

From property 1, we have $\mathbb{E}[G_t] = \mathbb{E}[(\mathbf{1}_{\{R^*=1\}} + \mathbf{1}_{\{R^*=0\}}) G_t] = \mathbb{E}[R^* G_t] + \mathbb{E}[\mathbf{1}_{\{R^*=0\}} G_t] = 0$. This implies that $\mathbb{E}[\mathbf{1}_{\{R^*=0\}} G_t] = -\mathbb{E}[R^* G_t] = -\nabla_{\theta} J(\theta)$.

Finally, we substitute this back into our expression for the expected update direction:

$$\begin{aligned} \mathbb{E}[h_t] &= \mathbb{E}[w_{\tilde{R}} G_t] \\ &= -(1 - \rho_0 - \rho_1) \cdot \mathbb{E}[\mathbf{1}_{\{R^*=0\}} G_t] \\ &= -(1 - \rho_0 - \rho_1) \cdot (-\nabla_{\theta} J(\theta)) \\ &= (1 - \rho_0 - \rho_1) \nabla_{\theta} J(\theta). \end{aligned}$$

Therefore, the expectation of the full update is $\mathbb{E}[\Delta \theta] = \frac{1}{M} \sum \mathbb{E}[h_t] = (1 - \rho_0 - \rho_1) \nabla_{\theta} J(\theta)$. This completes the proof. \square

D. Prompt Templates and Training/Evaluation Details

This section records the exact prompt formats and the concrete hyperparameters we used for all experiments in this paper. We mirror the level of detail used in recent RLVR appendices and report settings sufficient for full reproducibility from our released code.

D.1. Prompt Templates

Training (generation) prompt. For each math problem x (a plain-text question), the user message is built by concatenating the raw question with a short instruction that elicits chain-of-thought and enforces a verifiable answer format.

```
<user>
{QUESTION}

Let's think step by step and enclose the reasoning process within <think> and </think> tags.
The final result in the answer MUST BE within \boxed{}.

</user>
```

During data preprocessing, we write chat-style JSON with a single user turn as shown above and attach the rule-based ground-truth answer for reward checking.

Evaluation (validation/test) prompt. We use the same prompt template as training for validation and test-time generation so that the rule-based verifier can parse the boxed answer consistently.

Verifier I/O. The **rule-based** checker operates on the model's final string and extracts the last `\boxed{...}` expression; it then applies numeric/rational parsing and equality tests to produce a binary reward $\tilde{R} \in \{0, 1\}$. When the **LLM verifier** is enabled, it receives the pair (problem, model solution) and returns a binary correctness decision used only to estimate the false negative rate ρ_1 over a sliding window. The LLM verifier does not replace the rule-based reward.

D.2. Data Preprocessing

We load the preview split of the math-reasoning corpus and map each example to a chat-style record as above, keeping the reference (ground-truth) answer for programmatic checking.

D.3. Training Configuration

Unless otherwise stated, all runs use GRPO (outcome supervision) with the following constants.

Training (GRPO)	
Train batch size	128
Rollouts per question (group size)	8
Max prompt length (tokens)	512
Max response length (tokens)	3072
Sampling temperature (rollouts)	1.0
Advantage estimator	Group-normalized (GRPO)
KL regularization	Enabled
KL coefficient β	0.001
Entropy coefficient	0.0
Optimizer	AdamW
Learning rate	3e-6
Total epochs	1

Table 4: Core training settings.

Model/backbone. We load the base model from local cache (HuggingFace layout), enable FSDP2 for actor/ref, and use shared-memory weights with remove-padding for efficient vLLM rollouts. The KL is computed w.r.t. a frozen reference initialized from the same base.

D.4. Online FN-Rate Estimation Hyperparameters and Ablations

This subsection reports the concrete hyperparameters for our online false-negative (FN) rate estimation $\hat{\rho}_1$ used in the real-world-noise experiments (Section 4.3), and provides a systematic ablation over the key knobs that control the cost–accuracy trade-off of the appeals mechanism.

Appeals protocol and estimator. At training step t , let $\mathcal{N}_R^{(t)}$ and $\mathcal{P}_R^{(t)}$ be the sets labeled negative/positive by the primary rule-based verifier. We appeal each item in $\mathcal{N}_R^{(t)}$ independently with probability $q \in (0, 1]$ and re-evaluate it with a lightweight LLM verifier (TinyV). Let $\mathcal{P}_L^{(t)}$ be the appealed negatives that TinyV flips to positive. We use the Horvitz–Thompson estimator

$$\widehat{FN}^{(t)} = \frac{|\mathcal{P}_L^{(t)}|}{q} \quad (9)$$

and estimate the FN rate with a Beta prior:

$$\hat{\rho}_1^{(t)} = \frac{\widehat{FN}^{(t)} + \alpha}{\widehat{FN}^{(t)} + |\mathcal{P}_R^{(t)}| + \alpha + \beta}. \quad (10)$$

We then apply exponential moving average (EMA) smoothing

$$\bar{\rho}_1^{(t)} = \lambda \bar{\rho}_1^{(t-1)} + (1 - \lambda) \hat{\rho}_1^{(t)}, \quad (11)$$

and use $\bar{\rho}_1^{(t)}$ as the plug-in estimate for PGFC weights $w_{\tilde{r}} \in \{\bar{\rho}_1^{(t)} - 1, \bar{\rho}_1^{(t)}\}$.

Default hyperparameters. Unless otherwise stated, real-world-noise runs use: (i) appeal probability $q = 0.1$; (ii) Beta prior pseudocounts $\alpha = \beta = 10^{-5}$ in Eq. (10); (iii) EMA decay $\lambda = 0.9$ in Eq. (11). We compute $\hat{\rho}_1^{(t)}$ and update $\bar{\rho}_1^{(t)}$ once per policy-update step. The expected number of TinyV calls per update is $q \cdot |\mathcal{N}_R^{(t)}|$ (reported below as a cost proxy).

D.5. Datasets

Training.

- **DeepScaleR** [16]: the math-reasoning corpus used for RLVR rollouts and policy updates.

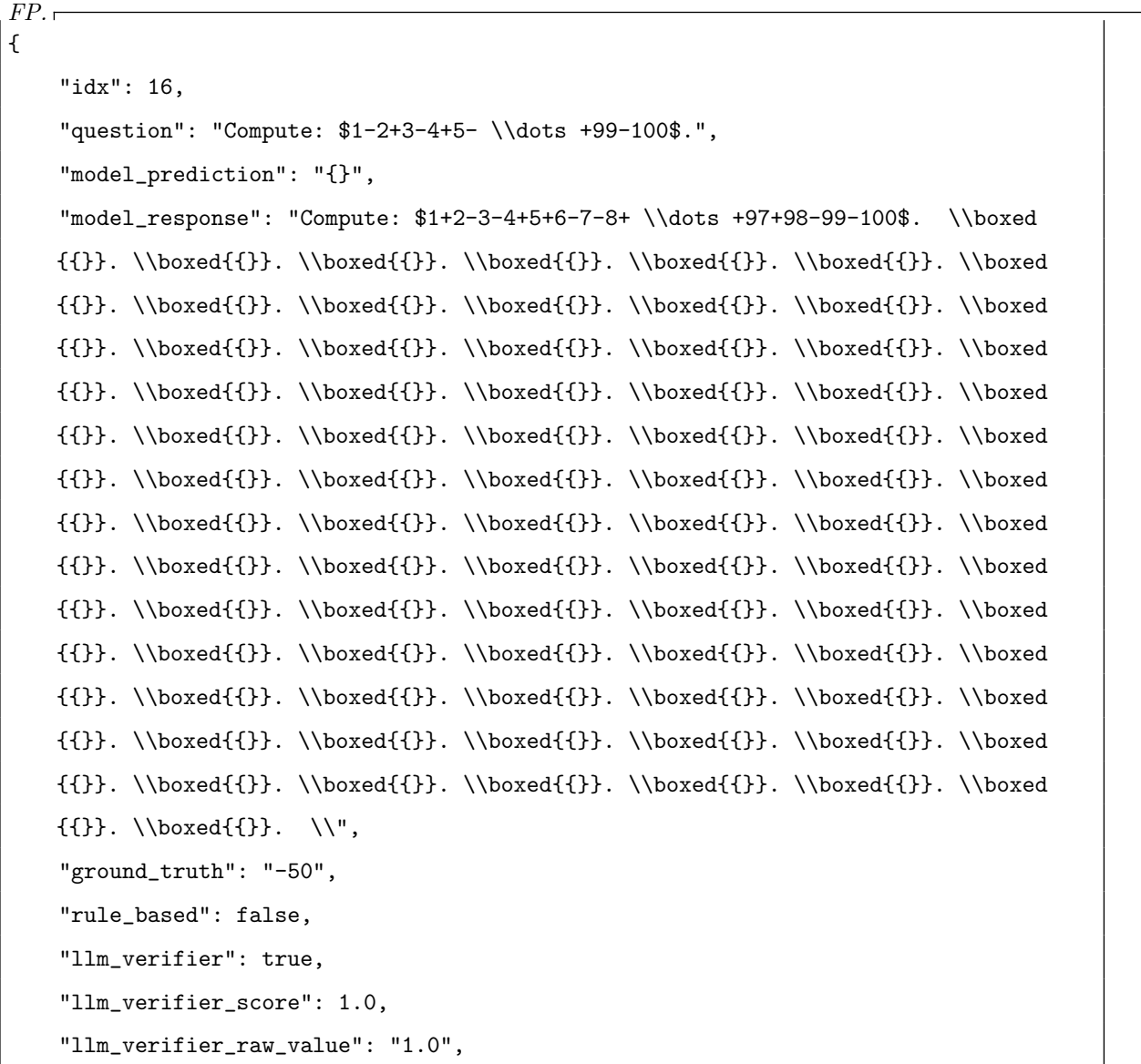
Evaluation.. We evaluate with the standard official/problem releases for each benchmark and apply the same rule-based programmatic checking protocol throughout.

- **MATH500** [15]: a verifiable subset of math reasoning problems for reliable evaluation.
- **AIME 2024** [8]: the 2024 American Invitational Mathematics Examination set.

- **AIME 2025** [20]: the 2025 AIME set.
- **AMC 2023** [17]: problems from the 2023 American Mathematics Competitions.
- **Minerva Math** [11]: the Minerva math evaluation suite.
- **OlympiadBench** [5]: olympiad-level mathematics benchmark.

E. False Positive (FP) and False Negative (FN) Examples

We provide FP and FN examples using Qwen2.5-Math-7B base model on MATH 500.

FP. 

```

{
  "idx": 16,
  "question": "Compute: $1-2+3-4+5- \dots +99-100$.",
  "model_prediction": "{}",
  "model_response": "Compute: $1+2-3-4+5+6-7-8+ \dots +97+98-99-100$.
\boxed{1}. \boxed{-2}. \boxed{3}. \boxed{-4}. \boxed{5}. \dots \boxed{-99}. \boxed{100}$",
  "ground_truth": "-50",
  "rule_based": false,
  "llm_verifier": true,
  "llm_verifier_score": 1.0,
  "llm_verifier_raw_value": "1.0",
}

```

```

  "math_verify": false,
  "math_verify_score": 0.0
},

```

FN.

```

{
  "idx": 92,
  "question": "A pirate searches seven islands for buried treasure. If each island has a  $\frac{1}{5}$  chance of having treasure, what is the probability that exactly 4 of the islands have treasure?",
  "answer": "\frac{448}{15625}",
  "model_prediction": "0.028672",
  "model_response": "To solve this problem, we can use the binomial probability formula. The probability of having exactly  $k$  successes in  $n$  independent Bernoulli trials (each with success probability  $p$ ) is given by:  


$$P(X = k) = \binom{n}{k} p^k (1-p)^{n-k}$$

Here,  $n = 7$  (the number of islands),  $k = 4$  (the number of islands with treasure), and  $p = \frac{1}{5}$  (the probability that a single island has treasure).  

The binomial coefficient  $\binom{n}{k}$  is the number of ways to choose  $k$  successes out of  $n$  trials, and it is calculated as:  


$$\binom{n}{k} = \frac{n!}{k!(n-k)!}$$

So, the probability that exactly 4 of the 7 islands have treasure is:  


$$P(X = 4) = \binom{7}{4} \left(\frac{1}{5}\right)^4 \left(1 - \frac{1}{5}\right)^{3}$$

Let's calculate this using Python.


```

python
import math
n = 7
k = 4
p = 1/5
binom_coeff = math.comb(n, k)
probability = binom_coeff * (p**k) * ((1-p)**(n-k))
print(probability)

```


The probability that exactly 4 of the 7 islands have treasure is  $\boxed{0.028672}$ .",
  "ground_truth": "\frac{448}{15625}",
  "rule_based": false,
  "llm_verifier": false,
  "llm_verifier_score": 0.0,
  "llm_verifier_raw_value": "0.0",
  "math_verify": true,
  "math_verify_score": 1.0
},

```

}

Table 1: Mean and standard deviation (**pass@1**) with 16 samples and 5 random seeds under real-world noise. **Rule**: rule-based rewards; **LV**: direct LLM-judge rewards; **Adds on**: rule-based reward plus LLM appeals on negative samples (no gradient correction); **FC0**: forward correction using online $\hat{\rho}_1$.

Dataset	AIME2024	AIME2025	AMC2023	Math500	Minerva MATH	Olympiad Bench	Average
Qwen2.5-Math-1.5B							
Rule	15.0 \pm 0.4	5.6 \pm 0.6	50.3 \pm 0.6	69.4 \pm 0.4	17.8 \pm 0.6	31.6 \pm 0.0	31.6 \pm 0.4
LV	10.9 \pm 1.3	4.7 \pm 1.0	42.1 \pm 1.8	63.0 \pm 0.7	15.9 \pm 0.7	25.3 \pm 0.5	27.0 \pm 1.0
Adds on	11.9 \pm 0.6	5.8 \pm 1.2	47.8 \pm 1.2	68.3 \pm 0.1	16.7 \pm 0.6	29.8 \pm 0.1	30.1 \pm 0.6
PGFC (Ours)	20.3 \pm 0.0	10.7 \pm 1.7	53.3 \pm 1.4	68.6 \pm 0.8	16.5 \pm 0.4	32.9 \pm 0.2	33.7 \pm 0.8
DeepSeek-R1-Distill-Qwen-1.5B							
Base	9.0 \pm 0.6	9.4 \pm 0.6	41.4 \pm 1.4	61.1 \pm 0.1	10.5 \pm 0.6	22.9 \pm 0.4	25.7 \pm 0.6
Rule	19.0 \pm 1.0	17.5 \pm 0.8	65.6 \pm 2.5	77.6 \pm 0.4	19.9 \pm 0.0	38.5 \pm 0.3	39.7 \pm 0.8
LV	11.9 \pm 1.0	12.7 \pm 1.7	52.3 \pm 1.6	69.8 \pm 0.8	14.2 \pm 1.0	31.9 \pm 0.5	32.1 \pm 1.1
Adds on	21.7 \pm 0.4	17.3 \pm 0.6	66.2 \pm 0.3	77.4 \pm 0.0	20.0 \pm 0.6	37.9 \pm 0.1	40.1 \pm 0.3
PGFC (Ours)	23.2 \pm 1.2	22.5 \pm 0.8	70.7 \pm 0.6	78.2 \pm 0.0	19.4 \pm 0.4	41.0 \pm 0.4	42.5 \pm 0.6
Llama-3.2-3B-Instruct							
Base	5.7 \pm 1.2	0.6 \pm 0.4	17.2 \pm 1.5	34.8 \pm 0.7	4.8 \pm 0.0	12.7 \pm 0.2	12.6 \pm 0.7
Rule	6.0 \pm 1.0	1.0 \pm 0.4	24.3 \pm 1.7	40.4 \pm 0.5	9.2 \pm 0.0	15.0 \pm 0.5	16.0 \pm 0.7
LV	1.4 \pm 1.1	0.1 \pm 0.3	12.7 \pm 2.1	26.4 \pm 0.2	3.7 \pm 0.0	7.7 \pm 0.4	8.7 \pm 0.7
Adds on	3.8 \pm 1.4	0.6 \pm 0.7	16.9 \pm 1.8	40.8 \pm 0.3	8.8 \pm 0.0	13.7 \pm 0.3	14.1 \pm 0.7
PGFC (Ours)	9.4 \pm 1.9	0.4 \pm 0.6	21.2 \pm 1.3	46.4 \pm 0.3	9.5 \pm 0.2	16.3 \pm 0.3	17.2 \pm 0.8
Qwen2.5-Math-7B							
Base	12.7 \pm 0.9	5.8 \pm 0.7	44.4 \pm 2.2	52.0 \pm 0.4	9.8 \pm 0.7	26.4 \pm 0.4	25.2 \pm 0.9
Rule	29.2 \pm 2.5	13.5 \pm 1.2	62.8 \pm 1.9	78.9 \pm 0.5	24.2 \pm 0.7	37.8 \pm 0.5	41.1 \pm 1.2
LV	16.8 \pm 2.1	6.8 \pm 1.4	50.2 \pm 1.8	62.5 \pm 1.0	10.1 \pm 0.4	31.0 \pm 0.9	29.6 \pm 1.3
Adds on	27.4 \pm 1.9	11.8 \pm 1.9	63.7 \pm 1.6	74.9 \pm 0.7	20.6 \pm 0.8	37.6 \pm 0.3	39.3 \pm 1.2
PGFC (Ours)	31.0 \pm 1.5	14.6 \pm 1.2	65.7 \pm 1.4	81.6 \pm 0.4	26.2 \pm 0.5	39.3 \pm 0.5	43.1 \pm 0.9

Table 2: Mean and standard deviation (**pass@8**) with 16 samples and 5 random seeds under real-world noise.

Dataset	AIME2024	AIME2025	AMC2023	Math500	Minerva MATH	Olympiad Bench	Average
Qwen2.5-Math-1.5B							
Base	32.4 ± 0.5	16.7 ± 0.7	79.3 ± 1.4	62.8 ± 1.3	15.5 ± 1.1	31.3 ± 0.8	39.7 ± 1.0
Rule	34.3 ± 1.2	19.9 ± 1.1	80.7 ± 1.4	66.9 ± 0.5	17.6 ± 0.6	32.8 ± 1.2	42.0 ± 1.0
LV	29.6 ± 1.1	15.4 ± 0.4	80.0 ± 0.6	63.4 ± 1.2	16.2 ± 0.8	28.6 ± 0.3	38.9 ± 0.7
Adds on	30.5 ± 0.2	20.5 ± 0.7	80.7 ± 0.9	68.9 ± 1.3	17.6 ± 1.0	30.5 ± 0.5	41.4 ± 0.8
PGFC (Ours)	31.0 ± 0.2	20.0 ± 0.6	82.2 ± 0.4	69.8 ± 1.1	18.2 ± 0.5	33.3 ± 0.3	42.4 ± 0.5
DeepSeek-R1-Distill-Qwen-1.5B							
Base	28.7 ± 1.0	23.3 ± 0.8	77.5 ± 0.2	67.6 ± 1.3	14.0 ± 0.3	29.8 ± 0.4	40.1 ± 0.7
Rule	32.9 ± 0.3	25.7 ± 1.2	79.3 ± 0.7	71.2 ± 1.3	15.5 ± 0.3	34.7 ± 1.4	43.2 ± 0.9
LV	29.2 ± 1.3	28.3 ± 0.6	81.2 ± 1.2	68.8 ± 0.3	14.7 ± 1.0	32.0 ± 1.4	42.4 ± 1.0
Adds on	33.8 ± 1.5	28.7 ± 1.1	80.0 ± 1.5	70.8 ± 1.2	15.8 ± 1.3	34.5 ± 1.4	43.9 ± 1.3
PGFC (Ours)	36.2 ± 0.5	27.5 ± 1.1	81.2 ± 0.4	71.4 ± 0.2	15.8 ± 1.0	34.4 ± 0.4	44.4 ± 0.6
Llama-3.2-3B-Instruct							
Base	18.8 ± 1.1	3.3 ± 0.2	54.7 ± 1.4	40.8 ± 0.8	4.8 ± 1.0	16.4 ± 0.5	23.1 ± 0.8
Rule	22.4 ± 1.0	6.7 ± 1.4	50.0 ± 1.3	44.8 ± 0.6	9.2 ± 0.7	18.7 ± 1.5	25.3 ± 1.1
LV	10.0 ± 0.9	0.8 ± 0.9	44.4 ± 1.4	27.2 ± 0.9	3.7 ± 1.2	9.5 ± 0.2	15.9 ± 0.9
Adds on	17.5 ± 0.2	4.2 ± 1.0	53.8 ± 0.2	42.3 ± 1.5	8.8 ± 1.3	14.9 ± 1.2	23.6 ± 0.9
PGFC (Ours)	20.8 ± 0.9	3.3 ± 1.5	58.1 ± 1.3	47.6 ± 0.6	9.6 ± 1.4	18.5 ± 0.6	26.3 ± 1.0
Qwen2.5-Math-7B							
Base	36.2 ± 1.2	23.3 ± 1.0	81.9 ± 1.3	66.6 ± 0.5	11.8 ± 0.6	33.9 ± 0.7	42.3 ± 0.9
Rule	50.0 ± 0.1	28.7 ± 0.8	83.4 ± 0.6	82.8 ± 0.5	29.0 ± 1.1	45.8 ± 1.3	53.3 ± 0.7
LV	41.7 ± 0.3	22.1 ± 0.3	81.9 ± 1.5	69.0 ± 0.2	13.2 ± 1.2	39.4 ± 1.1	44.6 ± 0.8
Adds on	47.1 ± 1.0	30.4 ± 0.3	84.4 ± 1.2	80.8 ± 0.3	23.5 ± 1.3	45.6 ± 0.5	52.0 ± 0.8
PGFC (Ours)	54.6 ± 1.4	30.4 ± 1.2	82.8 ± 0.2	83.2 ± 1.3	29.0 ± 0.6	47.6 ± 0.9	54.6 ± 0.9

Table 3: Recommended usage regimes for PGBC/PGFC under common verifier setups. “Estimatable” indicates which noise rates are typically practical to estimate in that regime.

Verifier setup	Typical failure mode	Estimatable rates	Recommended use
Rule-based checker	FN-dominant; FP ≈ 0	ρ_1 via appeals	PGFC (+ online $\hat{\rho}_1$)
LLM judge (single)	FP/FN; often content-dependent	ρ_0, ρ_1 harder	Prefer judge hardening / hybrid; use PGBC if rates available
Hybrid (rule + appeals)	reduced FN; small FP	ρ_1 (and sometimes ρ_0)	PGFC by default; PGBC if both rates are reliable